


Cite this: *RSC Adv.*, 2017, 7, 5694

# Nano KF/Al<sub>2</sub>O<sub>3</sub> particles as an efficient catalyst for no-glycerol biodiesel production by coupling transesterification

Ying Tang,\* Haomiao Ren, Feiqin Chang, Xuefan Gu and Jie Zhang\*

In this study, an efficient solid base catalyst, nano KF/Al<sub>2</sub>O<sub>3</sub>, for no-glycerol biodiesel production was prepared using nano  $\gamma$ -Al<sub>2</sub>O<sub>3</sub> particles as support, and was used in the tri-component coupling transesterification of canola oil, dimethyl carbonate and methanol. The preparation optimum conditions (blending temperature, blending time, calcination temperature and calcination time) as well as the loading amount of KF were screened in detail. A yield of biodiesel, 98.8%, was obtained under the conditions of KF loading of 10.0 wt%, calcination temperature of 400 °C, 2 h of reaction time at 338 K, 5.0 wt% catalysts and molar ratio of methanol/oil/DMC of 8 : 1 : 1. This high conversion of vegetable oil to biodiesel is considered to be associated with the high surface to volume ratio and basicity of the catalyst surface.

Received 25th October 2016  
Accepted 28th December 2016

DOI: 10.1039/c6ra25782h

www.rsc.org/advances

## Introduction

Biodiesel is a renewable fuel that can be produced from vegetable oils, animal fats, or recycled restaurant grease for use in diesel vehicles. Its physical properties are similar to those of petroleum diesel, but cleaner when being burnt, thus making biodiesel a good alternative fuel.<sup>1,2</sup> The prevailing method of biodiesel production in industry is transesterification of glycerol triglyceride with short-chain alcohols, such as methanol or ethanol, in the presence of soluble inorganic basic catalysts, such as sodium or potassium methoxides.<sup>3</sup> Although the reaction rates for this process are high, recovery of catalysts is difficult, and treatment of waste mixtures containing catalysts, water, glycerol and oils presents challenges. Problems can be reduced by using solid catalysts, which can be filtered off or centrifuged out of suspensions. However, heterogeneous catalysis produces glycerol<sup>4,5</sup> which needs an additional separation process, thus adding to the overall cost of biodiesel manufacture.<sup>6</sup> Glycerin is not very valuable as a by-product which simply adds to the over-supply of the commodity and thus contributes to a price depression.<sup>7</sup>

Generation of glycerol can be avoided through the reaction of vegetable oils and dimethyl carbonate (DMC) to produce glycerol carbonate (GC) as a secondary product, which does not require separation from the fatty acid esters.<sup>8</sup> A direct reaction between DMC and triglycerides can occur in the presence of sodium methoxide or potassium hydroxide (KOH) when refluxed at 90 °C for 6 h.<sup>9</sup> Ilham,<sup>10</sup> Saka<sup>11</sup> and Tan *et al.*<sup>12</sup> used DMC to produce biodiesel and GC at supercritical conditions in non-catalytic processes, while other researchers used enzymes to produce

biodiesel with DMC as reactant.<sup>13–15</sup> In our previous research, an indirect reaction between DMC and triglycerides has been established by adding methanol as the third reaction component.<sup>16</sup> Although the tri-component transesterification improved the reaction rate to a relatively high level, it still didn't reach the theoretical maximum due to low diffusion rate between the three-phase systems made up by the three components. Reaction can only occur on the interfacial region between phases, and the only way to increase yield is to increase contact area.<sup>17</sup> Our previous study focused on the use of nanocrystalline calcium oxides catalyst for the transesterification reaction,<sup>18</sup> and obtained high biodiesel yield of 99% at room temperature. The high catalytic activity of the nano-based catalyst was deduced from its high surface/volume ratio.

As we know now,  $\gamma$ -Al<sub>2</sub>O<sub>3</sub>-supported catalysts have shown high activity in heterogeneous reactions including transesterification for biodiesel production.<sup>19</sup> Yield of biodiesel can be greatly enhanced by the enormous increase of surface area of  $\gamma$ -Al<sub>2</sub>O<sub>3</sub>-supported nano materials. KF-impregnated commercial nanoparticles of  $\gamma$ -Al<sub>2</sub>O<sub>3</sub> have been used as heterogeneous catalysts for the transesterification of vegetable oil with methanol for the synthesis of biodiesel. In this paper, we present the results of nano KF/Al<sub>2</sub>O<sub>3</sub> catalyzed coupling transesterification of vegetable oil, dimethyl carbonate and methanol to produce biodiesel at moderate conditions. The catalytic activities and the effect of nano  $\gamma$ -Al<sub>2</sub>O<sub>3</sub> preparation condition on the yield of biodiesel were studied as well.

## Experiments

### Materials

Refined rapeseed or canola oil was purchased from Xi'an coal Co., Ltd. Dimethyl carbonate (DMC), methanol, analytical

College of Chemistry and Chemical Engineering, Xi'an Shiyou University, Xi'an, Shaanxi 710065, China. E-mail: tangying78@xsyu.edu.cn; zhangjie@xsyu.edu.cn



reagent grade, calcium carbonate (CC) (99% purity) and calcium oxalate monohydrate (CO) (98% purity) were purchased from Sinopharm Chemical Reagents Co., Ltd. (Beijing, China) and were used without further purification. Methyl heptadecanoate (gas chromatographic standard), nano  $\gamma$ - $\text{Al}_2\text{O}_3$  (95% purity) and surfactant OP-10 (octyl phenol with 10 moles per L of ethoxylate) were purchased from Sigma.

### Catalyst preparation

Nano  $\text{KF}/\gamma\text{-Al}_2\text{O}_3$  catalyst particles were prepared by the sol-gel method. Firstly, 5.0 g  $\gamma\text{-Al}_2\text{O}_3$  was added into 50 mL of ethanol, and then a certain amount of  $\text{KF}\cdot 2\text{H}_2\text{O}$  and 1 mL OP-10 was added in under stirring. The mixture was stirred for 2 h and a clear white gel was obtained. The white gel was kept at room temperature for 2 h. After that, the gel was heated up to 80 °C and kept for 2 h to vaporize water. Then the condensed gel was placed in a desiccator for 12 h to dry completely. The resulting dry gel was milled to white powder and calcinated under high temperature, and cooled to room temperature to complete the preparation procedure of catalyst  $\text{KF}/\gamma\text{-Al}_2\text{O}_3\text{-OP}$ . For comparison, the supported  $\text{KF}/\gamma\text{-Al}_2\text{O}_3$  was prepared by impregnating  $\text{KF}$  over commercial  $\gamma\text{-Al}_2\text{O}_3$  directly under same condition without ethanol.

### Materials characterizations

Thermo gravimetric analysis (TGA) of catalyst sample was performed in the static air condition 20–1000 °C with a heating rate of 5 °C  $\text{min}^{-1}$ , using a thermo-gravimetric analyzer/simultaneous differential thermal analyzer (TGA/SDTA 851<sup>c</sup>, Mettler-Toledo, Switzerland). Textural characteristics were investigated by means of surface area determined by BET including mean pore diameter and pore volume using desorption isotherms on a Micromeritics ASAP2000. The crystalline structures of the products of calcination were analyzed using an X-ray diffraction device (JDX-3530, JEOL, Japan) with an X-ray tube that has copper Cu as target and released  $\text{K}_\alpha$  radiation when accelerated at 30 mA and 40 kV. Scanning Electron Microscopy (SEM) was used for the investigation of surface morphology of catalyst samples. Before submitted to SEM characterization, the solid sample was coated with gold in order to achieve sufficient conductivity. Temperature-programmed desorption patterns of carbon dioxide ( $\text{CO}_2\text{-TPD}$ ) for the products were measured with an automated chemisorption analyzer (Autochem II 2920, Micromeritics, USA) at the temperature range from 40 to 800 °C with a heating rate of 10 °C  $\text{min}^{-1}$ .

### Preparation and analysis of biodiesel

Prior to reaction, the oil was treated with sodium hydroxide, at a ratio of 1 mg KOH per g lipids, and with bentonite to, respectively, lower fatty acid and water concentrations below 1 mg  $\text{g}^{-1}$  of triglyceride. The reaction was performed in a three necked round bottomed flask equipped with a reflux condenser and a thermometer. A certain amount of  $\text{KF}/\gamma\text{-Al}_2\text{O}_3$  and 8.01 g methanol were charged into the flask. Then 20.48 g rapeseed oil and 2.815 g DMC were added. The mixture was heated to and maintained at 65 °C with continuous stirring. Samples were

taken from the reaction mixture for each hour, and quenched to room temperature. The catalyst was separated by centrifugation, and the excess methanol was distilled off under vacuum. Samples were quantitatively analyzed for composition on an HP-6890 gas chromatograph equipped with a flame ionization detector and a fused-silica capillary column (HP-5; 0.32 mm  $\times$  30 m, 0.1  $\mu\text{m}$  film thickness) using methyl heptadecanoate as standard. The carrier gas was nitrogen with a flow rate of 20 mL  $\text{min}^{-1}$ . The oven temperature was kept constant at 280 °C. Yield was defined as a ratio of the weight of fatty acid methyl esters in samples, as determined using the GC, to the weight of equivalent fatty acid methyl esters contained in the oil used in the reaction.

## Results and discussion

### Characterizations of various samples

**Thermo-gravimetric analyses (TGA).** The thermal characteristics of support and the prepared  $\text{KF}/\gamma\text{-Al}_2\text{O}_3\text{-OP}$  and  $\text{KF}/\gamma\text{-Al}_2\text{O}_3$  samples were investigated using TGA from room temperature up to 1000 °C (Fig. 1). The weight losses in the range from 30 to 200 °C is due to loss of physically adsorbed water and hydroxyl from catalyst's surface, while the second weight loss step occurred at higher temperature in the TGA curve may be related to crystallization and/or weight loss due to components' loss of the catalysts caused by certain reactions occurring at high temperature.<sup>20</sup> It can also be found that the weight loss in the higher temperature range was enhanced over  $\text{KF}/\gamma\text{-Al}_2\text{O}_3\text{-OP}$  indicating the stronger interaction of support and  $\text{KF}$ .

**X-Ray diffraction analyses.** The X-ray diffraction patterns for support material  $\gamma\text{-Al}_2\text{O}_3$ ,  $\text{KF}/\gamma\text{-Al}_2\text{O}_3$  and  $\text{KF}/\gamma\text{-Al}_2\text{O}_3\text{-OP}$  are shown in Fig. 2. The plots show that all of samples have the characteristic peaks of  $\text{Al}_2\text{O}_3$  at  $2\theta$  of 37.0, 46.0 and 67.0. An additional  $\text{K}_2\text{O}$  phase can be observed in both catalysts with the characterization diffraction peak at 30.0, 42.7 and 53.0. The intensities of these peaks over  $\text{KF}/\gamma\text{-Al}_2\text{O}_3$  are not as high as those observed for  $\text{KF}/\gamma\text{-Al}_2\text{O}_3\text{-OP}$ , indicating the role of OP-

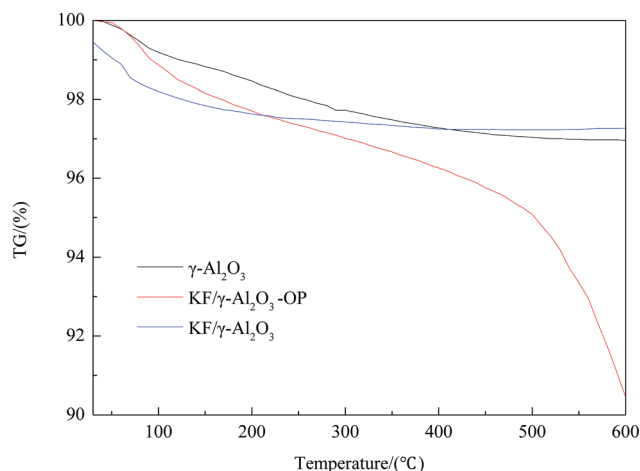


Fig. 1 TGA plot for  $\text{KF}/\gamma\text{-Al}_2\text{O}_3$  prepared by different method.



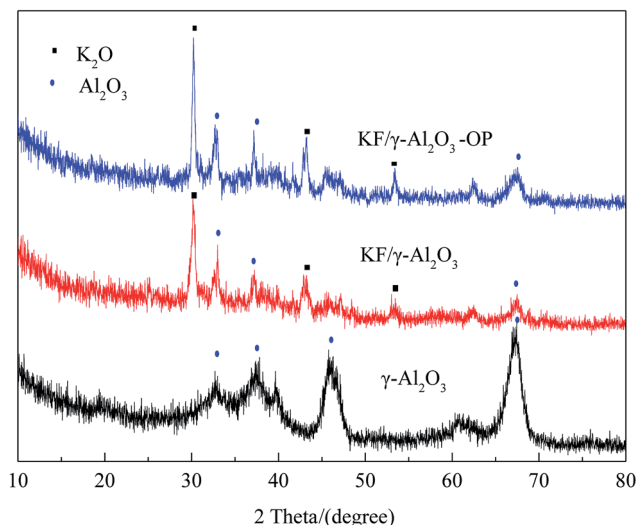


Fig. 2 XRD patterns for  $\gamma$ - $\text{Al}_2\text{O}_3$  and  $\text{KF}/\gamma$ - $\text{Al}_2\text{O}_3$  prepared by different method.

10 to improve the dispersion of  $\text{Al}_2\text{O}_3$  in the mixture as suggested previously. Studies have discovered the relationship of the high catalytic activity of  $\text{KF}$ -impregnated alumina catalysts with the basicity of the surfaces, which is due to the formation of the  $\text{K}_2\text{O}$  and  $\text{Al-O-K}$  groups derived from the thermal decomposition of the loaded  $\text{K}$  compounds by salt-support interactions.<sup>21</sup>

**Surface properties.** The BET surface, pore size and average pore volume of  $\text{KF}/\gamma$ - $\text{Al}_2\text{O}_3$  obtained from different method are characterized and listed in Table 1. As shown in Table 1, the specific surface area  $S_{\text{BET}}$  of  $\gamma$ - $\text{Al}_2\text{O}_3$  decreased greatly from  $396.3 \text{ m}^2 \text{ g}^{-1}$  to  $278.5 \text{ m}^2 \text{ g}^{-1}$  after supporting  $\text{KF}$  with a large reduction of pore volume, whereas the BET surface area for  $\text{KF}/\gamma$ - $\text{Al}_2\text{O}_3$ -OP still remains a high value of  $389.9 \text{ m}^2 \text{ g}^{-1}$ . This may be due to its smaller particle size and/or smaller pore diameter caused by second calcination under high temperature. The surface area and pore properties of  $\text{KF}/\gamma$ - $\text{Al}_2\text{O}_3$ -OP were greatly enhanced compared with  $\text{KF}/\gamma$ - $\text{Al}_2\text{O}_3$ , reflecting a significant role of ethanol as surfactant to prevent aggregation of nano- $\text{Al}_2\text{O}_3$  during preparation. Nitrogen adsorption-desorption isotherms obtained with all of the samples are shown in Fig. 3. The nitrogen adsorption isotherms of  $\gamma$ - $\text{Al}_2\text{O}_3$  and  $\text{KF}/\gamma$ - $\text{Al}_2\text{O}_3$  exhibit the typical type III isotherm, indicating that all of the samples were macroporous, and a low energy of adsorption as well. The capillary condensation of  $\text{N}_2$  can be observed at relative high pressure.

Table 1 Pore structure properties of the catalyst

| Sample   | BET surface area ( $\text{m}^2 \text{ g}^{-1}$ ) | Pore volume ( $\text{cm}^3 \text{ g}^{-1} \times 10^{-2}$ ) | Pore size (nm) |
|--|--|---|----------------|
| $\gamma$ - $\text{Al}_2\text{O}_3$               | 396.34   | 0.9054  | 91.3801        |
| $\text{KF}/\gamma$ - $\text{Al}_2\text{O}_3$ -OP | 389.97   | 0.7230  | 75.3185        |
| $\text{KF}/\gamma$ - $\text{Al}_2\text{O}_3$     | 278.46   | 0.4328  | 50.3287        |

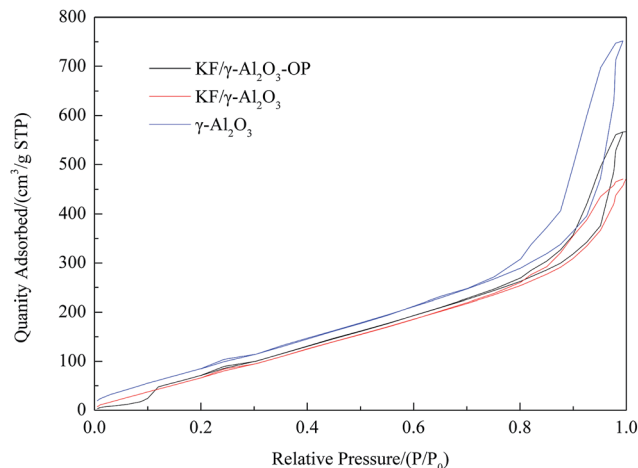


Fig. 3 Nitrogen adsorption curves of  $\gamma$ - $\text{Al}_2\text{O}_3$  and  $\text{KF}/\gamma$ - $\text{Al}_2\text{O}_3$  prepared by different method.

**Basic properties.** For solid basic catalysts, the amount of irreversibly adsorbed  $\text{CO}_2$  reflects the population of base sites on exposed surfaces. The desorption temperature indicates the strength of adhesion at the base site. Results for temperature-programmed desorption were presented in Fig. 4. The profiles exhibit peaks between  $400^\circ\text{C}$  and  $700^\circ\text{C}$  associated with strong base for transesterification reaction.<sup>22</sup> The broad band associated with weak or medium strength interactions of  $\text{CO}_2$  with the basic sites on catalyst particles moves to almost below  $200^\circ\text{C}$ , indicating the weak basic sites. In the samples,  $\text{KF}/\gamma$ - $\text{Al}_2\text{O}_3$ -OP showed higher and broader desorption peak around  $600$ – $650^\circ\text{C}$  attributed to the strong basic sites of  $\text{O}^{2-}$  anions, whereas  $\text{KF}/\gamma$ - $\text{Al}_2\text{O}_3$  showed a considerably smaller desorption peak with the maximum temperature of  $598^\circ\text{C}$ . Consistent with previous findings,<sup>23</sup> the increased surface area and the basicity of the catalysts will benefit to their activities, so the FAME yield may be increased directly with increasing basicity of the high catalyst surface over  $\text{KF}/\gamma$ - $\text{Al}_2\text{O}_3$ -OP.

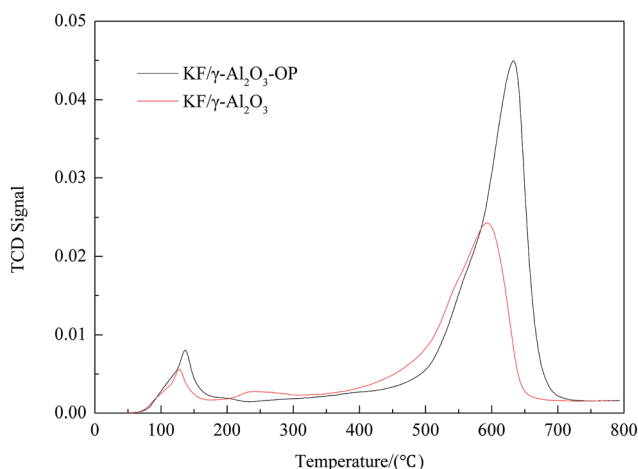


Fig. 4  $\text{CO}_2$ -TPD curves of  $\text{KF}/\gamma$ - $\text{Al}_2\text{O}_3$  prepared by different method.



**Scanning electron microscopy (SEM).** The SEM image of  $\gamma$ - $\text{Al}_2\text{O}_3$ ,  $\text{KF}/\gamma\text{-Al}_2\text{O}_3\text{-OP}$  and  $\text{KF}/\gamma\text{-Al}_2\text{O}_3$  were shown in Fig. 5. These graphs showed a good dispersion of KF on the surface of  $\gamma\text{-Al}_2\text{O}_3$ , however, the surface morphology has been changed over  $\text{KF}/\gamma\text{-Al}_2\text{O}_3$  and some degree of agglomeration is evident from the large particles. It was further confirmed that the dispersion function of ethanol during the preparation of  $\text{KF}/\gamma\text{-Al}_2\text{O}_3$  using nano- $\gamma\text{-Al}_2\text{O}_3$  as support. It can be found that the particle size of  $\text{KF}/\gamma\text{-Al}_2\text{O}_3$  was smaller than that of  $\text{KF}/\gamma\text{-Al}_2\text{O}_3\text{-OP}$  while the surface area of latter was larger. Generally, an inverse proportionality between BET area and particle size was deduced based on geometry. However, for the macroscopic material that may have been more capacity potentially leading to an artificial increase in the specific surface area, and a change in the apparent surface reactivity.<sup>24</sup>

### Effect of preparation parameters

**Effect of the amount of KF.** As suggested by previous reports that  $\text{K}_2\text{O}$  was the main active sites for the transesterification of supported KF catalysts, hence a series of  $\text{KF}/\gamma\text{-Al}_2\text{O}_3\text{-OP}$  catalyst calcined at  $400^\circ\text{C}$  for 2 h with loaded KF ranging from 0.5–3.0 mmol  $\text{g}^{-1}$  have been investigated under  $65^\circ\text{C}$  at 2 h. Fig. 6 shows very high FAME yield as high KF loading amount, indicating the enhanced activity due to a concomitantly remarkable increase in surface basicity. In order to obtain the best catalytic performance, more KF were loaded under same reaction condition and achieved 98.8% of FAME yield for the  $\text{KF}(10\%)/\gamma\text{-Al}_2\text{O}_3\text{-OP}$ , but the yield declined as KF amount exceeding 10.0%. These differences may be associated with the strong basic sites resulted from KF loading on  $\text{Al}_2\text{O}_3$ , which can also be covered by the excess KF. Drawing on the results, the optimum loading amount of KF was selected as 10.0%.

**Effect of blending time.** The dispersion of hydrophobic  $\text{Al}_2\text{O}_3$  particles in the KF solution was greatly influenced by the amount of surfactant, OP-10, employed during the process of catalyst preparation. The optimum blending time for the preparation of supported  $\text{Al}_2\text{O}_3$  was determined by performing reaction at varying reaction time in the range of 1–3 h. The experimental results, reported in Fig. 7 indicated that the FAME yield increased with blending time between 1 h and 2 h of complete mixing, while long blending time caused low yield, probably due to increasing viscosity. Thus, the maximum FAME yield of 98.8% was achieved after 2 h of blending time.

**Effect of blending temperature.** In order to improve the solution of OP-10, blending temperature during catalyst

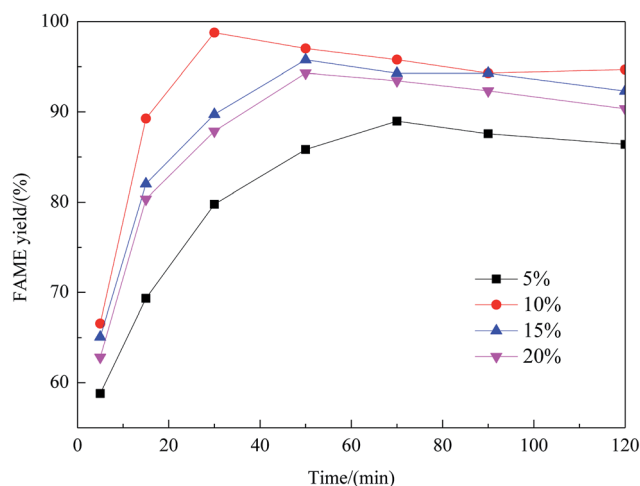


Fig. 6 Effect of amount of KF on the performance of  $\text{KF}/\gamma\text{-Al}_2\text{O}_3\text{-OP}$ .

preparation process was screened in the temperature range from  $60$  to  $75^\circ\text{C}$  and summarized in Fig. 8. From the result, it was believed that the relatively high blending temperature improved the mutual oil-methanol-DMC miscibility, resulting in an increase of the FAME yield. The maximum FAME yield of 98.8% was achieved when the mixture was stirred at  $65^\circ\text{C}$ . However, extremely high blending temperature caused a decrease in the yield of FAME, which possibly owing to

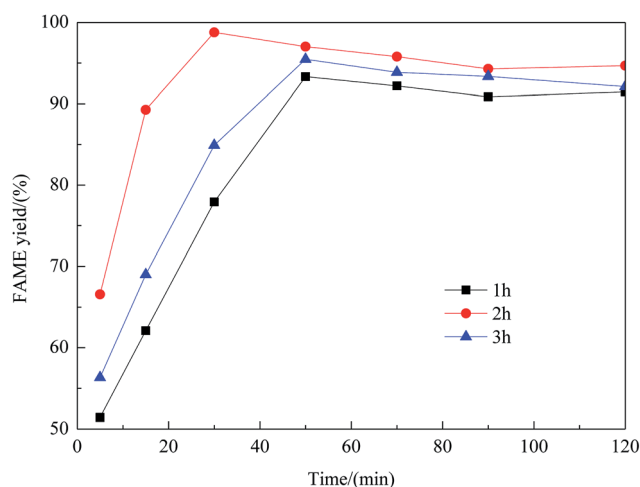


Fig. 7 Effect of blending time on the performance of  $\text{KF}/\gamma\text{-Al}_2\text{O}_3\text{-OP}$ .

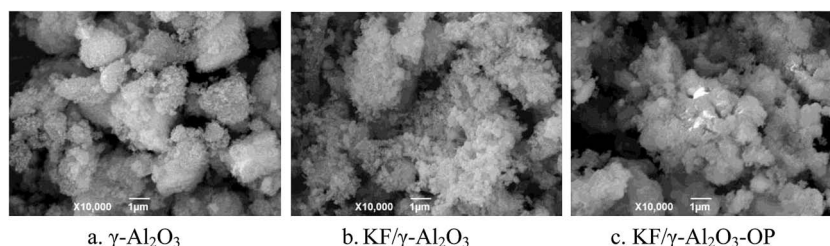


Fig. 5 SEM photographs of  $\gamma\text{-Al}_2\text{O}_3$  and  $\text{KF}/\gamma\text{-Al}_2\text{O}_3$  prepared by different method.



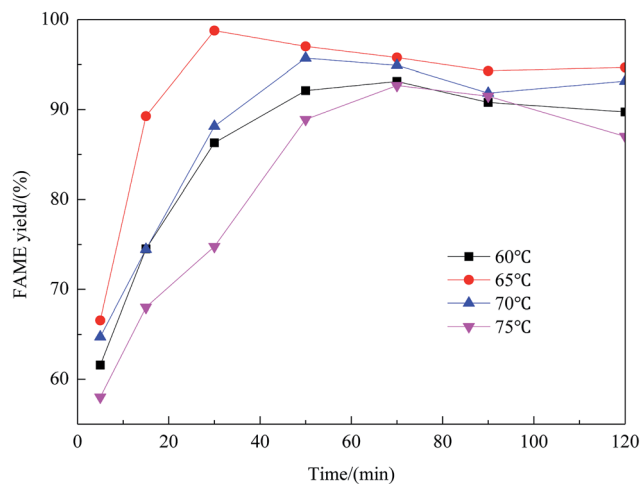


Fig. 8 Effect of blending temperature on the performance of KF/γ-Al<sub>2</sub>O<sub>3</sub>-OP.

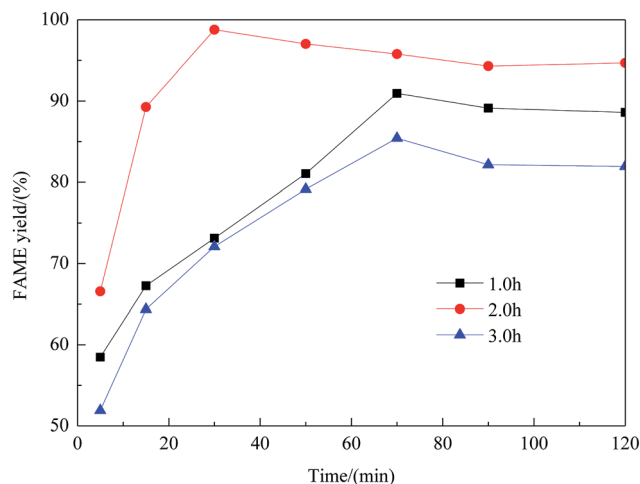


Fig. 10 Effect of calcination time on the performance of KF/γ-Al<sub>2</sub>O<sub>3</sub>-OP.

a miscibility problem involving OP-10 and Al<sub>2</sub>O<sub>3</sub> particles under high temperature. Accordingly, the preparation condition for nano-KF/γ-Al<sub>2</sub>O<sub>3</sub> was studied under blending temperature of 65 °C.

**Effect of calcination temperature.** As we are aware, the calcination temperature plays an important role in the catalytic activity of solid catalyst by producing much active site of mixed oxides and the KF decomposition extent. Therefore, the KF/γ-Al<sub>2</sub>O<sub>3</sub>-OP was calcined at different temperature (200 °C, 300 °C, 400 °C and 500 °C) in order to seek for better activity. From the results summarized in Fig. 9, it can be found that the yield of FAME increased with calcination temperature until 400 °C, which contributed to the appearance of basic active site from the decomposition of KF, and the maximum FAME yield of 98.8% can be obtained over the catalyst calcined at 400 °C. However, slight descending of FAME yield appeared when further increasing calcination temperature to 500 °C. This was possibly due to agglomeration of catalyst surface area and loss

of potassium species by sublimation or penetration into the subsurface, an influential factor for the reaction rate especially for the heterogeneous reaction.

**Effect of calcination time.** Since the activity variation of KF/γ-Al<sub>2</sub>O<sub>3</sub>-OP catalyst should be attributed to the distribution of potassium on the alumina support which were calcined at different time, the calcination time of KF/γ-Al<sub>2</sub>O<sub>3</sub>-OP was investigated from 1 h to 3 h. From the results summarized in Fig. 10, it can be concluded that an appropriate calcination time was at 400 °C for 2 h to obtain the maximum FAME yield of 98.8%. Overlong calcination time caused the decrease of yield of FAME due to loss of active sites as a result of agglomeration of catalyst surface. Therefore, calcination time of 2 h was suitable for obtaining high yield of FAME.

**Effect of reaction parameters.** Transesterification was preceded using three components of rapeseed oil, methanol and DMC at mild conditions as our previous publication referred.<sup>17</sup> Methanol first reacted with the triglyceride to produce FAME and glycerol. In the coupling process, the

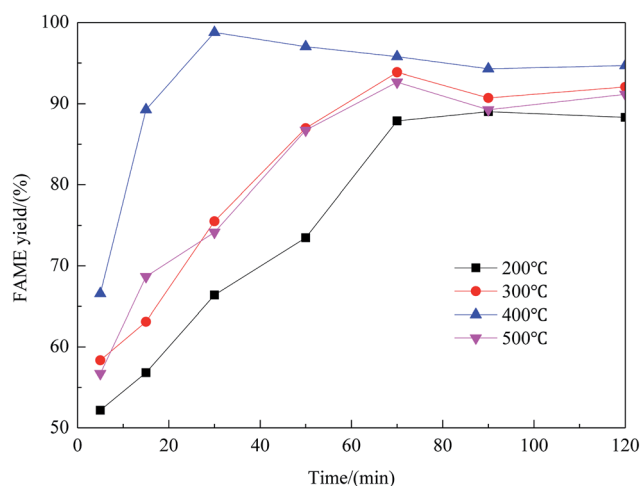


Fig. 9 Effect of calcination temperature on the performance of KF/γ-Al<sub>2</sub>O<sub>3</sub>-OP.

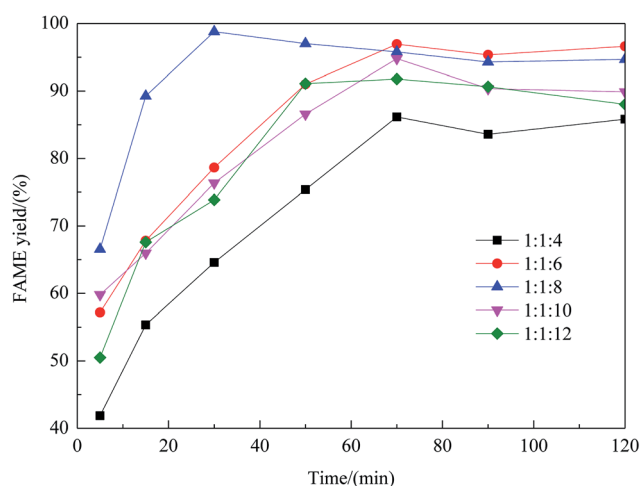


Fig. 11 Effect of molar ratio on the performance of KF/γ-Al<sub>2</sub>O<sub>3</sub>-OP.



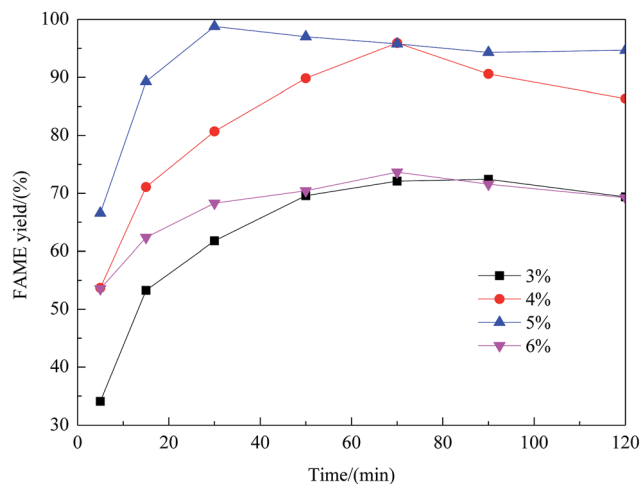


Fig. 12 Effect of catalyst content on the performance of KF/γ-Al<sub>2</sub>O<sub>3</sub>-OP.

produced glycerol reacted with dimethyl carbonate to form glycerol carbonate and methanol. From prior work, the optimal proportion of the feed reactants, on a molar basis, was 1 : 1 : 8 of oil : DMC : methanol under refluxing. For obtaining maximum reaction rate of the transesterification process, an overall optimization is necessary, and the reaction parameters which affect the yield of FAME have been itemized in detail.

**Effect of molar ratio.** As we know, the transesterification reaction between rapeseed oil and methanol generally requires a large excess of methanol to shift the equilibrium favorably, so the molar ratio of methanol to oil should be investigated. Fig. 11 graphically illustrates the FAME yield changing with the molar ratio of methanol to oil, under 1 : 1 molar ratio of rapeseed oil to DMC. As shown in this figure, with an increase of the methanol amount, the yield of FAME enhanced considerably. The maximum yield of FAME, 98.8%, was obtained as the molar ratio reached 8 : 1. However, beyond the molar ratio of 8 : 1, excessive methanol caused the yield to decrease, which was possibly due to the mixing difficulty caused by mass transfer hindrance involving excess reactants, products and solid catalyst. Therefore, the optimum molar ratio of methanol to rapeseed oil was determined as 8 : 1.

**Effect of catalyst amounts.** The dependence of the yield of FAME on the catalyst amount was studied in the presence of KF-γ-Al<sub>2</sub>O<sub>3</sub>-OP at 65 °C. The catalyst amount varied in the range

Table 3 The produced fuel properties over KF/γ-Al<sub>2</sub>O<sub>3</sub>-OP

| Fuel property               | Unit                            | Prepared FAME | EU (EN14214) |
|-----------------------------|---------------------------------|---------------|--------------|
| Density (15 °C)             | g mL <sup>-1</sup>              | 0.88          | 0.86–0.90    |
| Kinematic viscosity (40 °C) | mm <sup>2</sup> s <sup>-1</sup> | 3.18          | 3.5–5.0      |
| Pour point                  | °C                              | –9.4          | —            |
| Cold filter plugging point  | °C                              | –10.0         | —            |
| Flash point                 | °C                              | 144.0         | ≥101         |
| Free glycerol               | % (m m <sup>-1</sup> )          | 0.018         | <0.02        |

of 3.0–6.0% (w/w) of oil. The reaction profile summarized in Fig. 12 indicated that the FAME yield was strongly dependent with catalyst percentage. Due to insufficient active sites, low addition of catalyst was unable to lead to high yield of FAME until it reached to 5.0%. While increased reaction rate can be observed in initial reaction time, indicating relatively high activity of supported catalyst. When the amount of catalyst increased from 3% to 5%, the yield of FAME at 30 min increased from 62.1% to 98.8%. Further increase in the catalyst amount led to the decrease of the yield of FAME. The reason for this decreasing trend was the mixing problem in presence of high amount of catalyst, which increased the viscosity of the reactants and lowered the yield of FAME. This result also implied that the transesterification of KF-γ-Al<sub>2</sub>O<sub>3</sub>-OP was strongly dependent on the amount of basic sites.

### The comparison study

The catalytic performances of KF-γ-Al<sub>2</sub>O<sub>3</sub>-OP for biodiesel production with or without DMC have been investigated, and the properties of the product were studied. As presented in Table 2. Nearly 98.9% yield of FAME was obtained within 30 min using the proposed coupling transesterification under the optimized condition (65 °C, 1 : 1 : 8 molar ratio of methanol, oil to DMC), while transesterification between methanol and rapeseed oil resulted in 96.5% yield of FAME within 70 min. The main reason for high FAME yield over KF-γ-Al<sub>2</sub>O<sub>3</sub>-OP containing DMC should be contributed to the integration of two transesterifications of methanol/rapeseed oil and glycerol/DMC, which resulted in promoting the transesterification between rapeseed oil and methanol towards the favored direction as suggested in our previous results. As a result, the

Table 2 Catalytic performance of prepared catalysts

| Reaction condition          | Unit | KF/γ-Al <sub>2</sub> O <sub>3</sub> -OP |           | KF/γ-Al <sub>2</sub> O <sub>3</sub> |
|-----------------------------|------|---|-----------|-------------------------------------|
|                             |      | Without DMC                             | With DMC  | With DMC                            |
| Reaction time               | min  | 70                                      | 30        | 120                                 |
| Reaction temperature        | °C   | 65                                      | 65        | 65                                  |
| Molar ratio                 | —    | 1 : 8                                   | 1 : 1 : 8 | 1 : 1 : 8                           |
| Amount of catalyst          | %    | 5                                       | 5         | 5                                   |
| Yield of FAME               | %    | 96.5                                    | 98.8      | 37.3                                |
| Yield of glycerol carbonate | %    | —                                       | 98.6      | 37.2                                |



conversion of rapeseed oil was enhanced by activating and converting glycerol to glycerol carbonate, which shifted the transesterification of methanol and rapeseed oil favorably to give high FAME yield. The comparison study on the catalytic activity of  $\text{KF}/\gamma\text{-Al}_2\text{O}_3\text{-OP}$  and  $\text{KF}/\gamma\text{-Al}_2\text{O}_3$  was carried out under the optimum reaction condition obtained above:  $65^\circ\text{C}$ ,  $1:1:8$  molar ratios of oil/DMC/methanol, 5 wt% of catalyst. From this study it can be seen that the yield of FAME was enhanced to near to 98.8% in the presence of  $\text{KF}/\gamma\text{-Al}_2\text{O}_3\text{-OP}$  at 30 min, while with  $\text{KF}/\gamma\text{-Al}_2\text{O}_3$  it needed 120 min to obtain only 37.3%. In view of the characteristic results of the catalysts, it is obvious that the activity change of the catalysts was well correlated to the change of their basicity. Besides, the surfactant can also improve the dispersion of active species over support as it greatly enhanced the forming of both  $\text{K}_2\text{O}$  species and  $\text{Al-O-K}$  groups in the composite.

### The quality of produced oil

For the aim of being commercial applicable, the produced biodiesel must be characterized using specified analytical methods to ensure it meeting the international standards. Therefore, some properties, including viscosity, density, flash point and free glycerol value were investigated and listed in Table 3. The specifications of both biodiesel are close to the European standard, EN14214 and the literature data.<sup>25</sup> It should be noted that the free glycerol in biodiesel obtained from the new method is within the range of European standard, thus indicates that the coupling transesterification eliminated glycerol efficiently as we suggested before. The viscosity of obtained biodiesel is lower than the limit of EN14214 due to the presence of glycerol derivatives, and this property may improve the spray injection behavior of the fuel.

### Conclusion

In this research, nano- $\text{KF}/\gamma\text{-Al}_2\text{O}_3$  was prepared by blending powdered nano- $\gamma\text{-Al}_2\text{O}_3$  with an aqueous solution of  $\text{KF}$  followed by calcination at a high temperature in air. The dispersed nano- $\gamma\text{-Al}_2\text{O}_3$  increased the surfactivity greatly, and the  $\text{K}_2\text{O}$  species formed during the thermal decomposition of loaded  $\text{KF}$  was probably the main reason for the high catalytic activity. Nearly 99.0% yield of FAME was obtained within 30 min using the proposed coupling transesterification under the optimized condition ( $65^\circ\text{C}$ ,  $1:1:8$  molar ratio of methanol, oil to DMC). Furthermore, the reaction reduced the free glycerol content in biodiesel product to make it a great advantage of avoiding the risk of plug in fuel filters.

### Acknowledgements

This work was financially supported by grants from Natural Science Research Plan Projects of Shaanxi Science and

Technology Department (2016JM2012), National Natural Science Foundation of China (21306149).

### References

- 1 Q. Liu, R. R. Xin and C. C. Li, *J. Environ. Sci.*, 2013, **25**, 823–829.
- 2 A. J. Dassey, S. G. Hall and S. Chandra, *Algal Res.*, 2014, **4**, 89–95.
- 3 F. Ma and M. A. Hanna, *Bioresour. Technol.*, 1999, **70**, 1–15.
- 4 J. Bone, J. Coata, S. Romain, J. S. Reneaume, A. E. Plesu and V. Plesu, *Food Bioprod. Process.*, 2009, **111**, 773–778.
- 5 G. El Diwani, N. K. Attia and S. I. Hawash, *Int. J. Environ. Sci. Technol.*, 2009, **6**, 219–224.
- 6 G. J. Van, *Fuel Process. Technol.*, 2005, **86**, 1097–1107.
- 7 D. T. Johnson and K. A. Taconi, *Environ. Prog.*, 2007, **26**, 338–348.
- 8 D. Delledonne, F. Rivetti and U. Romano, *Appl. Catal., A*, 2001, **221**, 241–251.
- 9 D. Fabbri, V. Bevonni, M. Notari and F. Rivetti, *Fuel*, 2007, **86**, 690–697.
- 10 Z. Ilham and S. Saka, *Bioresour. Technol.*, 2009, **100**, 1793–1796.
- 11 S. Saka and Y. Isayama, *Fuel*, 2009, **88**, 1307–1313.
- 12 G. T. Ang, K. T. Tan and K. T. Lee, *Renewable Sustainable Energy Rev.*, 2014, **31**, 61–70.
- 13 P. J. Seong, B. W. Jeon, M. Lee, D. H. Cho, D. K. Kim, K. S. Jung, S. W. Kim, S. O. Han, Y. H. Kim and C. Park, *Enzyme Microb. Technol.*, 2011, **48**, 505–509.
- 14 L. P. Zhang, S. Z. Sun, Z. Xin, B. Y. Sheng and Q. Liu, *Fuel*, 2010, **89**, 3960–3995.
- 15 Y. M. Ji and E. Y. Lee, *Biotechnol. Lett.*, 2011, **33**, 1789–1796.
- 16 Y. Tang, Q. T. Cheng, H. Cao, L. Zhang, J. Zhang and H. F. Li, *C. R. Chim.*, 2015, **18**, 1328–1334.
- 17 G. Wen, Z. F. Yan, M. Smith, P. Zhang and B. Wen, *Fuel*, 2010, **89**, 2163–2165.
- 18 M. L. Granados, *Appl. Catal., B*, 2006, **3**, 317–326.
- 19 K. Noiroj, P. Intarapong, A. Luengnaruemitchai and S. Jai-In, *Renewable Energy*, 2009, **34**, 1145–1150.
- 20 K. Naemchanthara, S. Meejoo and W. Onreabroy, *Adv. Mater. Res.*, 2008, **55**, 333–336.
- 21 M. J. Ramos, A. Casas, L. Rodríguez, R. Romero and Á. Pérez, *Appl. Catal., A*, 2008, **346**, 79–85.
- 22 X. Deng, Z. Fang, Y. H. Liu and C. L. Yu, *Energy*, 2011, **36**, 777–784.
- 23 H. Li, S. L. Niu and C. M. Lu, *Fuel*, 2016, **176**, 63–71.
- 24 C. K. Lambert and R. D. Gonzalez, *Microporous Mater.*, 1997, **12**, 179–188.
- 25 C. S. Castro, L. C. F. G. Júnior and J. M. Assaf, *Fuel Process. Technol.*, 2014, **125**, 73–78.

